Microfilament dynamics during cell movement and chemotaxis monitored using a GFP–actin fusion protein

Monika Westphal, Andreas Jungbluth, Manfred Heidecker, Bettina Mühlbauer, Christina Heizer, Jean-Marc Schwartz, Gerard Marriott and Günther Gerisch

Background: The microfilament system in the cortex of highly motile cells, such as neutrophils and cells of the eukaryotic microorganism *Dictyostelium discoideum*, is subject to rapid re-organization, both spontaneously and in response to external signals. In particular, actin polymerization induced by a gradient of chemoattractant leads to local accumulation of filamentous actin and protrusion of a 'leading edge' of the cell in the direction of the gradient. In order to study the dynamics of actin in these processes, actin was tagged at its amino terminus with green fluorescent protein (GFP) and observed with fluorescence microscopy in living cells of *D. discoideum*.

Results: Purified GFP–actin was capable of copolymerizing with actin. In the transfected cells of *D. discoideum* studied, GFP–actin made up 10–20% of the total actin. Microfilaments containing GFP–actin were capable of generating force with myosin in an *in vitro* assay. Observations of single living cells using fluorescence microscopy showed that the fusion protein was enriched in cell projections, including filopodia and leading edges, and that the fusion protein reflected the dynamics of the microfilament system in cells that were freely moving, being chemotactically stimulated, or aggregated. When confocal sections of fixed cells containing GFP–actin were labeled with fluorescent phalloidin, which binds only to filamentous actin, there was a correlation between the areas of GFP–actin and phalloidin fluorescence, but there were distinct sites in which GFP–actin was more prominent.

Conclusions: Double labeling with GFP–actin and other probes provides an indication of the various states of actin in motile cells. A major portion of the actin assemblies visualized using GFP–actin are networks or bundles of filamentous actin. Other clusters of GFP–actin might represent stores of monomeric actin in the form of complexes with actin-sequestering proteins.

Address: Max-Planck-Institut für Biochemie, D-82152 Martinsried, Germany.

Correspondence: Günther Gerisch
E-mail: gerisch@vms.biochem.mpg.de

Received: 2 December 1996
Revised: 17 January 1997
Accepted: 17 January 1997

Published: 12 February 1997
Electronic identifier: 0960-9822-007-00176

Current Biology 1997, 7:176–183

Background

The goal of the work described in this paper was to study the dynamics of actin assembly and disassembly in highly motile cells, and to correlate re-organization of the actin cytoskeleton with changes in cell shape. In order to visualize actin, we have used cells of *Dictyostelium discoideum* which permanently produce a fusion protein of actin and the green fluorescent protein (GFP) from *Aequorea victoria*. GFP has been shown to be an appropriate tag for determining not only the localization of various proteins within living cells, but also the dynamics of their redistribution in response to external signals [1–6]. In yeast cells, an actin–GFP fusion protein integrates into cortical actin patches that move in an energy-dependent manner [7].

Undeveloped single cells of *D. discoideum* are characterized by a continuous protrusion and retraction of pseudopodia from any part of their surface [8,9]. The chemotactic orientation of aggregating cells is dominated by the chemoattractant-induced polymerization of actin [10]. Cells quickly respond to a change in the direction of a cyclic AMP (cAMP) gradient by retracting existing pseudopodial extensions, and a few seconds later by extending filopodia and lamellipodia in the direction of the new gradient, creating a new cell front. In the course of aggregation, the cells become integrated into streams, where they attach to each other in a head-to-tail arrangement [11]. Cell-to-cell adhesion in the streams suppresses independent cell movement.

We report here on the dynamics of actin redistribution under conditions of unbiased cell motility or chemotactic stimulation, and on the stabilization of actin assembly at the site of head-to-tail adhesion. In living cells, actin

Figure 1

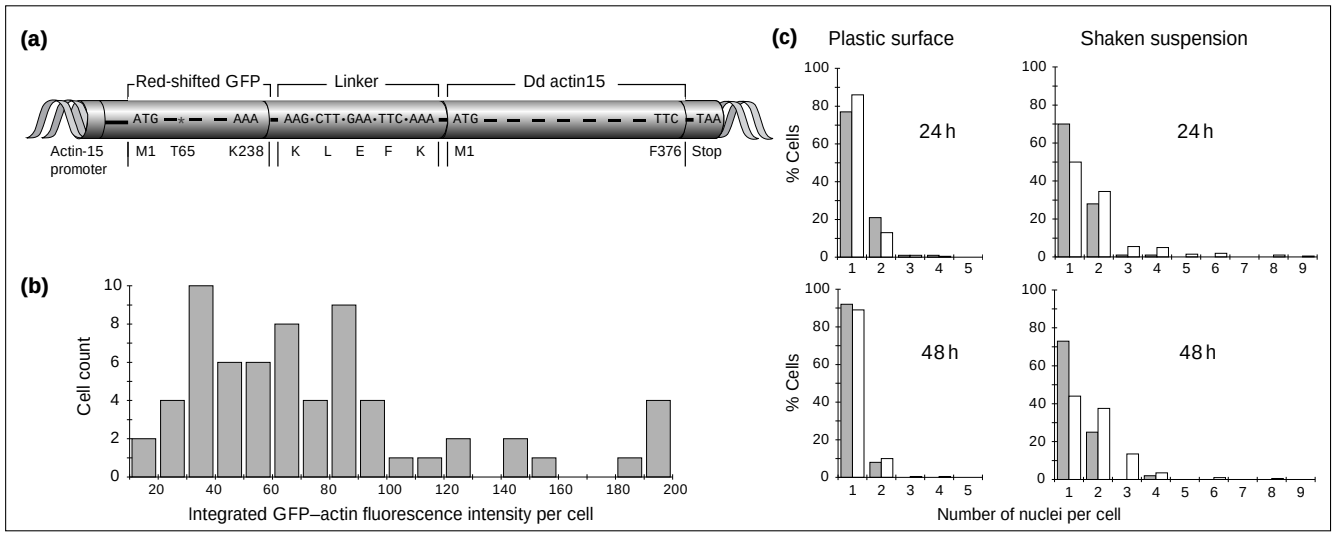

GFP–actin production in cells of *D. discoideum*. (a) The GFP–actin construct. The actin-15 promoter that drives transcription is active in growing and early developing cells. The transcript encodes a fusion protein comprising GFP at its amino terminus and actin at its carboxyl terminus, with a 5 amino-acid linker in between. The encoded actin sequence is that of the major actin form of *D. discoideum* [35], which is the common translation product of the actin 8 and 15 genes [36]. The first and last amino acids of GFP and actin, as well as those of the linker peptide, are indicated (lower line), as are the nucleotides encoding them (middle line). Also indicated is the position of the point mutation (T65) in red-shifted GFP (asterisk, middle line). (b) Histogram of fluorescence intensity of individual cells cultivated in petri dishes with nutrient medium, washed and then measured in phosphate buffer; the intensity is given in arbitrary units. (c) Histograms showing numbers of nuclei in wild-type cells (grey bars) and in cells expressing GFP–actin (white bars). At the beginning of the experiment, cells were harvested from plastic petri dishes, and 3×10^5 cells per ml were inoculated into nutrient medium, either in plastic dishes (left) or in shaken suspension (right). After 24 h, samples of cells were fixed and stained with DAPI to count nuclei (24 h time point). At the same time point, each culture was diluted again to 3×10^5 cells per ml with fresh medium and cultivated for another 24 h as before (48 h time point). Nuclei in 98–210 cells were counted for each cell type and condition. Differences between normal and GFP–actin-producing cells were analyzed using the Mann–Whitney test. For the 24 h values in shaken suspension, $p = 0.07$. Differences between the other distributions of normal and GFP–actin-producing cells were not significant ($p > 0.2$).

occurs in the form of either filaments of polymerized actin (F actin) or monomers (G actin) probably bound to actin-sequestering proteins. A few studies have reported that unpolymerized actin also exists in the form of complexes located close to cell regions undergoing dynamic re-organization [12,13]. Regional differences in the state of actin were investigated in the work described here by combining confocal microscopy of GFP–actin with labeling of actin filaments by cyanine 5–phalloidin (Cy5–phalloidin).

Results

D. discoideum cells producing GFP–actin

The coding region of *D. discoideum* actin was fused at its 5′ end to the coding sequence of the red-shifted GFP S65T mutant, which contains a serine to threonine substitution at residue 65 [14]. These sequences were linked to each other by an oligonucleotide encoding a five amino-acid peptide, which acts as a short spacer between the amino-terminal GFP and the carboxy-terminal actin moieties (Fig. 1a). Transcription of the GFP–actin sequence was driven by the actin-15 promoter. *D. discoideum* AX2 cells were transfected with this construct, and transformants were selected with G418. To quantify the amount of the fusion protein, western blots of total cell lysates were probed with a monoclonal antibody recognizing the carboxy-terminal region of *D. discoideum* actin. The transfected cells produced an average of 6% GFP–actin fusion protein relative to endogenous actin. The distribution of fluorescence intensities in transfected cells was quite broad, with about 10% of cells having GFP–actin fluorescence intensity three-fold higher than the mean (Fig. 1b).

D. discoideum cells expressing the GFP–actin gene were only slightly impaired in functions associated with the actin system; they were capable of moving, growing by the uptake of bacteria, aggregating and developing into fruiting bodies. Mitotic cell division was not detectably affected when the cells were cultivated in contact with a plastic surface. A slight impairment of cytokinesis was indicated, however, by an increase in the proportion of binucleate and multinucleate cells during growth in suspension (Fig. 1c); this type of growth provides a rigorous test for the capacity of mutant cells to divide normally [15,16].

Motility of copolymers of actin and GFP–actin *in vitro*

In order to test the ability of GFP–actin to polymerize into filaments, GFP–actin was copurified with actin from transfected *D. discoideum* cells. In the richest fraction,

Figure 2

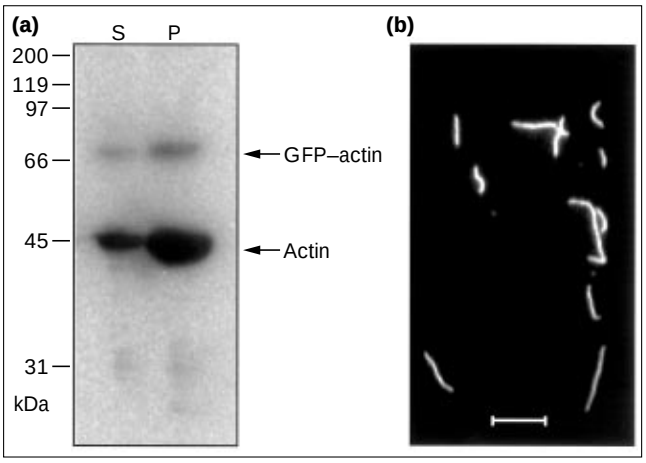

Copolymerization of GFP–actin with endogenous actin from *D. discoideum* cells. (a) A fraction containing both free actin and the fusion protein was incubated in polymerization buffer and subjected to high-speed centrifugation at 100 000 *g*. Supernatant (S) and pellet (P) fractions were analyzed by immunoblotting with [^{125}I]-labeled anti-actin 236 antibody. (b) Copolymerization with normal actin results in filaments visible by their intrinsic GFP fluorescence. The scale bar indicates 10 μm. Single phalloidin-stabilized actin filaments containing 30% GFP–actin were bound on a surface of heavy meromyosin in the absence of ATP. The GFP fluorescence of the filaments was imaged with an intensified charge-coupled device camera operating at 25 frames per second for 1 sec. The image shown is an average of these 25 frames. The velocity of similar filaments in an *in vitro* motility assay was measured in the presence of 1 mM ATP [23].

GFP–actin represented about 70% of the total actin. With a 1:1 mixture of normal *D. discoideum* actin and GFP–actin, no significant changes in fluorescence intensity were seen during polymerization of G actin. The fluorescence excitation and emission maxima in this fraction, 488 nm and 511 nm, respectively, were consistent with the spectral properties of GFP S65T [14].

Assays *in vitro* confirmed that the GFP–actin fusion protein preserved the basic functions of actin, although some quantitative differences were evident. GFP–actin copolymerized with normal actin in physiological salt and depolymerized after dialysis against a low-salt buffer (G buffer). The ratio of GFP–actin to actin in the polymerized fraction was about half the ratio in the unpolymerized fraction; from the western blot shown in Figure 2a, actual GFP–actin to actin ratios of 0.07 and 0.13 were estimated for the supernatant and pellet, respectively.

Single actin filaments, containing 0, 15, 30, 50 or 70% GFP–actin, were capable of binding to heavy meromyosin in the rigor state and were visualized in the *in vitro* motility assay [17]. Single actin filaments containing 30% or more GFP–actin and stabilized with non-fluorescent phalloidin could be visualized through their own GFP fluorescence (Fig. 2b). GFP–actin-containing filaments stabilized with phalloidin coupled to tetramethyl rhodamine isothiocyanate (TRITC) showed a strong resonance energy transfer from the GFP moiety to the TRITC group. The sliding velocity for the 0 and 15% GFP–actin-containing filaments visualized using the fluorescence of bound TRITC–phalloidin was within the range 3.2–4.0 μm sec^{-1}, with all filaments moving smoothly. Filaments containing 30% GFP–actin moved with a velocity of 3.0–3.5 μm sec^{-1}. Some of these filaments were seen to stop for a few seconds and then to continue movement, and occasional severing of filaments was observed. Most filaments containing 50% GFP–actin were capable of moving at a velocity of about 3 μm sec^{-1}, although there was an increase in the frequency of pausing and extensive filament severing. Only a small fraction of filaments containing 70% GFP–actin were capable of moving (at 2.0–2.5 μm sec^{-1}), and this motility was limited to just a few seconds. On the basis of these results, we conclude that actin filaments containing up to 70% GFP–actin are capable of forming a rigor complex with heavy meromyosin, and that GFP–actin molecules in the filament significantly interfere with the activity of the myosin motor only when their content exceeds 30%.

Actin dynamics in freely moving and aggregating cells

In freely moving cells, a bright GFP fluorescence was seen in filopodia and lamellipodia attached to the substratum and in crown-shaped extensions of the upper cell surface (Fig. 3a–c). These thin or flat cell projections with a thickness of less than 1 μm are known to be packed with actin filaments [18,19]. The timecourse shown in Figure 3d–k illustrates a brightly labeled cell which rounded up after 20 seconds and then changed its direction by extending a new leading edge. At all stages of this time series, active protrusion of leading edges was associated with elevated local levels of GFP–actin. A control using GFP S65T showed diffuse cytoplasmic labeling without any accumulation at specific sites (data not shown), as previously reported for wild-type GFP [2,3].

After the assembly of aggregating cells into streams, actin is concentrated primarily at the front of each cell, at the site of its contact with the preceding cell [20]. The distribution of GFP–actin was in line with these published observations obtained by phalloidin labeling of fixed cells. The time series shown in Figure 3l–q reveals that this localization was stabilized as long as cells were contiguous. Images from this time series show that in the brighter, trailing cell, GFP–actin was concentrated at the site of cell–cell contact. Towards the middle of this sequence, the trailing cell became less polarized and eventually reversed its direction, although during the entire manoeuvre the GFP–actin remained concentrated at the site of cell–cell contact.

Actin reassembly in chemotactic responses

A *D. discoideum* cell stimulated by cAMP through a micropipette turns towards the source of chemoattractant

in one of two ways: either by bending the front of the cell into the direction of the gradient, or by collapse of the pseudopodia at the existing front, followed within seconds by the protrusion of a new front from the cell surface nearest the source [21]. Monitoring of GFP–actin revealed the dynamics of actin assembly and disassembly during a long chemotactic response (Fig. 4). During their movement in a cAMP gradient, cells alternated between phases of pseudopod extension and more rounded states, and GFP–actin accumulated and dissipated at the front of each cell in phase with the switches.

Overlap between sites of GFP–actin accumulation and phalloidin labeling

In order to see whether the equilibrium between G and F actin in a motile cell is reflected in the distribution of GFP–actin, cells moving on a glass surface were fixed and labeled with Cy5–phalloidin, which marks only F actin. As was seen in living cells, a fraction of the GFP–actin in fixed cells was uniformly distributed in the cytoplasm, but was excluded from the nucleus and other organelles (Fig. 5a,d,g). This diffuse cytoplasmic GFP–actin is most likely to indicate monomeric GFP–actin. In addition to the diffuse cytoplasmic signal, a bright GFP–actin fluorescence was observed at the cell cortex. In superimposed images of phalloidin and GFP–actin fluorescence, areas of high GFP–actin accumulation coincident with intense phalloidin labeling appear in pseudocolor as yellow/orange (Fig. 5c,f,i). In general, these areas were the most intensely labeled with phalloidin (Fig. 5b,e,h), and they obviously represent GFP–actin polymerized into filaments. There were, however, also areas in the cortical regions of the cells that were predominantly green (for example, see Fig. 5i). The significance of these poorly overlapping regions is discussed below.

Discussion

Actin-based motility with a GFP–actin load

The use of GFP–actin in this study made it possible to monitor the dynamics of actin accumulation and disassembly in living, highly motile cells, and thus to focus on the temporal aspect that is omitted when phalloidin- or antibody-labeled preparations of fixed cells are analyzed. By using cells permanently producing GFP–actin instead of cells microinjected with labeled actin, cell injury is avoided and no recovery period is required. The fluorophore of GFP S65T was chosen because of its high extinction coefficient, resistance to photobleaching, and respectable quantum yield obtained with blue–green excitation [22]. For future applications, the absence of the 396 nm absorption band when using GFP S65T–actin will free a wavelength 'window' for the selective excitation of a blue fluorescent protein fusion, for example a fusion with an actin-binding protein, which may be used to map actin interactions with other proteins dynamically, in live cells, using fluorescence-energy transfer image microscopy [23,24].

Figure 3

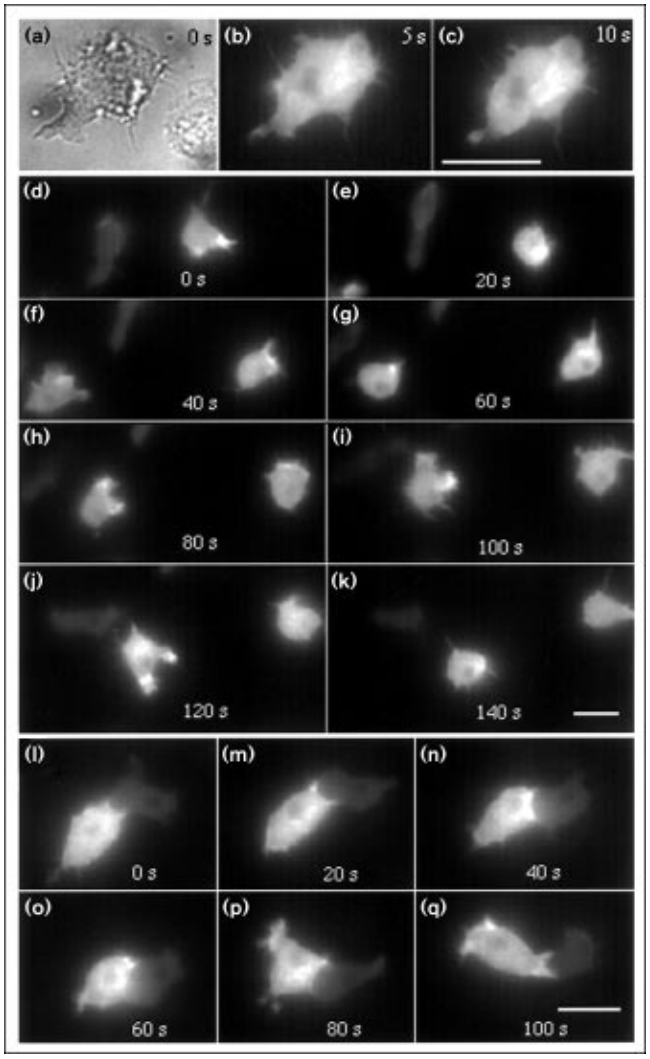

(a–k) Redistribution of GFP–actin to protrusions of the surface of cells moving over glass, and **(l–q)** stabilization of actin assembly at a site of cell-to-cell contact. (a) A transmission image and (b,c) fluorescence images of a cell were taken at intervals of 5 sec. This highly fluorescent cell had numerous filopodia labeled with GFP–actin. Comparison of the two fluorescence images (b,c) reveals the dynamic protrusion and retraction of filopodia. (d–k) Time series of GFP–actin fluorescence images of moving cells with largely varying intensities of GFP–actin fluorescence. The two brightest cells reveal how GFP–actin redistributes to discrete areas of the cell cortex when cells change from a more rounded shape to one actively protruding leading edges. Fluorescent filopods are most clearly seen in (k). (l–q) Time series of GFP–actin in a two-cell stream. The two cells aggregating in tandem were distinguished by low (cell on the right) and high (cell on the left) fluorescence intensities. Nuclei are recognizable as dark areas in the fluorescence images of the cells. Cells had been starved for (a–c) 1 h or (d–k) 5.5 h to record them at pre-aggregation stages, or (l–q) for 6 h to record them at the beginning of aggregation. Images were recorded with an exposure time of 0.2 sec; the scale bars indicate 10 μm.

The ability of GFP–actin to incorporate into actin filaments was not unexpected; as seen in the model of the actin filament made by Holmes *et al.* [25], the amino

Figure 4

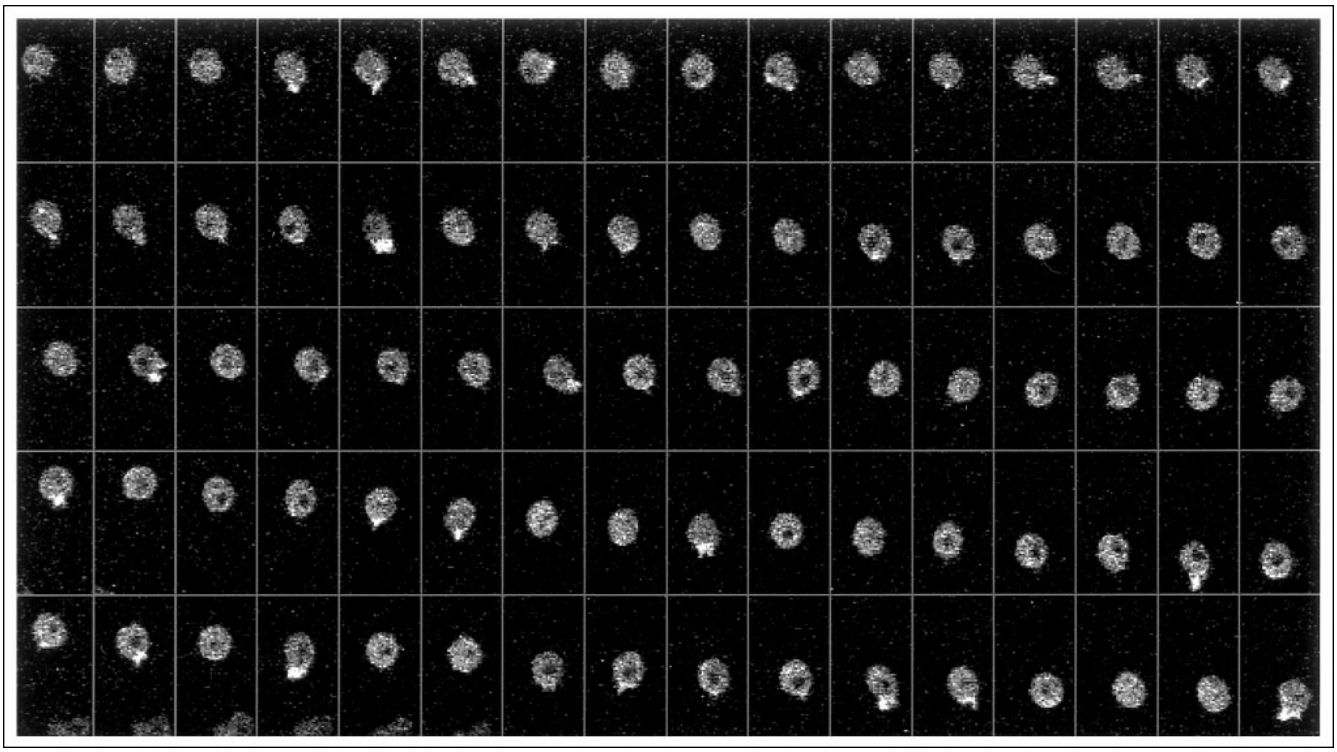

GFP–actin dynamics during a chemotactic response. The sequence (left to right, continuing on successive lines) shows confocal sections through a strongly fluorescing cell on its path to a micropipette filled with cAMP. The cell moved in a shallow diffusion gradient from a distance of 111 μm at the beginning of the sequence over a length of 82 μm towards the source of the chemoattractant. Images were taken every 20 sec and the width of each frame corresponds to 25 μm.

terminus of actin is not located at a subunit–subunit interface. More surprising was the finding that actin filaments containing up to 70% GFP–actin were capable of binding to myosin (Fig. 2b). Structural models reveal that portions of the amino terminus of actin are in contact with myosin heads in the rigor state [26] and presumably also during the actomyosin ATPase cycle [27]. Filaments containing up to 30% GFP–actin exhibited an almost normal sliding velocity and motility behavior in the *in vitro* motility assay. Filaments containing more than 30% GFP–actin exhibited deficiencies in sliding motion, such as increased pausing and severing. The most likely explanation of our motility data is that, although myosin can bind to GFP–actin molecules in the filament, it can only produce a power stroke when bound to unmodified actin molecules in the filament. According to this explanation, increasing the content of GFP–actin decreases the probability of unmodified actin molecules engaging in a power stroke, forcing myosin to work against a GFP–actin load and resulting in either no net movement or severing of filaments. The growth of cells producing GFP–actin in suspension culture with only marginal impairment of cytokinesis indicates that GFP–actin does not substantially interfere with the actin–myosin interactions *in vivo*. In contrast, cells in which the function of myosin II is suppressed form giant multinucleated cells in suspension culture, so their cytokinesis must be much more impaired [15,16].

We have also tested GFP fused to the carboxyl terminus of actin, but obtained only weak expression with no distinct localization of the fusion protein to specific structures within cells (our unpublished observations). In yeast, a linker of at least 10 amino acids is necessary to prevent GFP fused to the carboxyl terminus of actin from severely affecting cell function [7].

Rapid assembly and dissipation of actin at leading edges

One of the most attractive applications for GFP–actin is in correlating the assembly and disassembly of actin with changes in shape and behavior of rapidly moving cells (Fig. 3d–k). This use of GFP–actin can be exploited in *D. discoideum*, using mutants to establish the interplay between actin-associated proteins in the regulation of cell motility.

Observing GFP–actin during a time series of *D. discoideum* cells moving in a gradient of chemoattractant reveals details of the stimulus–response coupling which could not be documented by any other currently available method.

Figure 5

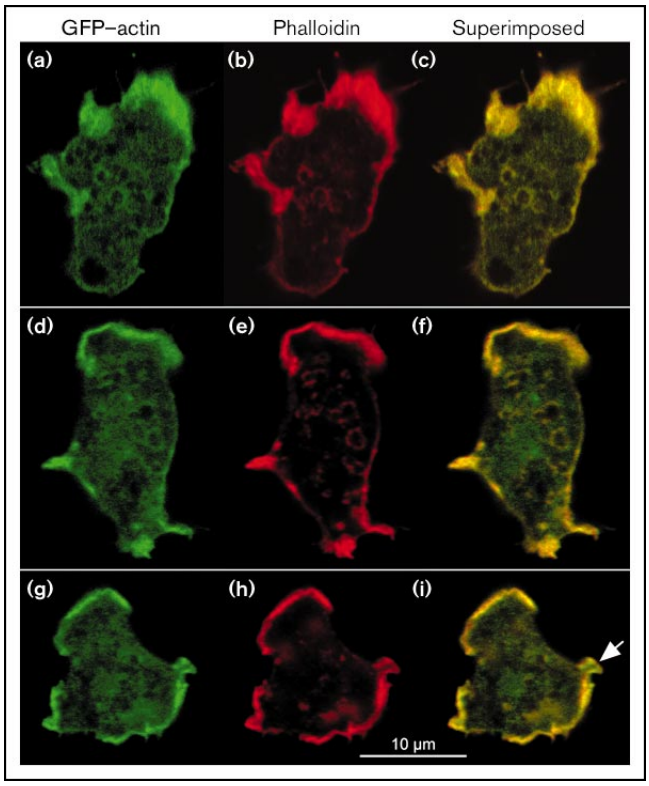

GFP–actin fluorescence compared to phalloidin labeling. In confocal sections of fixed cells, the fluorescence emission of GFP–actin (a,d,g) and Cy5-labeled phalloidin (b,e,h) were recorded, and the two images were superimposed (c,f,i). Green areas on the superimposed image indicate a predominance of the GFP signal; such areas are detectable in the cortical region (for instance, the surface extension indicated by the arrow) and at sporadic patches within the cytoplasm: most distinct are the two spots in (f). Cy5-labeled phalloidin was used in order to avoid energy transfer from GFP to TRITC–phalloidin.

Differences in fluorescence intensity of GFP-labeled actin in a single cell reflect the fluctuations of receptor-mediated actin assembly near to the site on the cell surface facing the micropipette tip which acts as the source of attractant. A weak response, associated with uncertainties about orientation, is observed in cells positioned far away from the micropipette (Fig. 4). This response is characterized by the local 'firing' of actin assembly and its frequent interruption by phases of less polarized actin distribution. The switches often occurred during the 20 second interval between image recordings in our time series. These results indicate that processes that control the local assembly of actin are subject to rapid 'on and off' switching during biased movement in a continuous gradient of chemoattractant. Previous findings suggest that actin co-assembles with a number of accessory proteins in response to chemoattractant: the new fronts elicited by chemoattractant are known to be populated within seconds by at least two actin-associated proteins, coronin [2] and talin [28].

When, during the course of movement of a cell along a gradient, the chemotactic input becomes consistently stronger, the off switches are effectively suppressed. The cell then consistently moves with a stable front pointing towards the micropipette (Fig. 4). A similar stabilization of local actin assembly is seen at sites of cell-to-cell adhesion (Fig. 3l–q). It is tempting to speculate that the signals elicited by chemoreceptor stimulation might converge at the same cytoskeletal targets as the transmembrane effects of cell adhesion proteins.

Are actin clusters at the cell cortex always filamentous?

The most straightforward explanation for the enrichment of GFP–actin in the cell cortex is that it polymerizes into filaments that form a network associated with the plasma membrane. Phalloidin is a specific label for F actin. One would expect, therefore, that areas of the cell cortex that are enriched in GFP–actin coincide with phalloidin-labeled regions. Although this is generally true, Figure 5 shows that there are local differences in intensities of the GFP and phalloidin signals. These differences may be due either to phalloidin binding only a fraction of the F actin accumulated at the cell cortex, or to the assembly of G actin, presumably with sequestering proteins, into large, non-filamentous complexes. Evidence for the first possibility comes from the demonstration that phalloidin cannot interact with cofilin-decorated F-actin [29]. Support for the second possibility is provided by the finding that sequestered G actin forms patches in fibroblasts [13] and sea urchin embryos [12]. Candidates for G-actin-binding proteins in *D. discoideum*, which might store G actin for rapid polymerization, are profilins I and II [30] and CAP [31].

Materials and methods

Vector construction and cell transformation

A vector for expression of the GFP–actin fusion in cells of *D. discoideum* under the control of the actin 15 promoter was constructed from the transformation vector pDEX H [32]. The insert contained a continuous reading frame composed of, first, the coding sequence of GFP from *A. victoria* in which the serine 65 residue was converted to threonine using a PCR strategy; second, a pentapeptide linker, which results from the cloning procedure; and third, the entire coding sequence and 50 base pairs of 3′-flanking sequence, including a polyadenylation signal, of an actin cDNA clone. The cDNA clone was obtained by screening a library from *D. discoideum* AX3 with the actin-specific antibody 224-236-1 ('236'). The cDNA gives rise to the same translation product as the Dd actin 8 and 15 genes. The entire insert was blunt-end ligated into the *Hin*dIII site of the pDEX H vector, and the vector introduced into the genome of *D. discoideum* AX2 cells using electroporation. Transformants were selected on plates in nutrient medium containing 20 μg ml^{-1} G418. The transformant clone HG1662 was used for all experiments; cells producing free GFP S65T were used as a control.

Cell culture

Cells of *D. discoideum* AX2, whether wild type or transformants producing either GFP–actin or GFP, were routinely cultivated axenically in 10 ml liquid medium in polystyrene petri dishes (90 mm diameter) at near confluent densities (about 2×10^6 cells per ml). For transfected cells, G418 was added to a final concentration of 20 μg ml^{-1}. In order

to count nuclei, cells were cultivated, in parallel, in petri dishes and in suspension culture rotary shaken at 150 r.p.m. The cells were fixed at –20°C in methanol, and the nuclei stained with 4′,6′ diamido-2-phenylindole hydrochloride (DAPI). As constituents of the nutrient medium sensitized the cells to light, for the experiment shown in Figure 4, cells were cultivated on SM agar plates with *Klebsiella aerogenes*; cells were then scraped from the fringe of a colony, washed and starved in 17 mM potassium/sodium-phosphate buffer, pH 6.0 ('starvation buffer').

Fluorescence microscopy of living cells and chemotaxis assays

D. discoideum cells round up when exposed to intense irradiation with blue or near-ultraviolet light [33]. In order to minimize light sensitivity of the cells as a result of extrinsic chromophores, such as those derived from pinocytosis of culture medium, it proved preferable to grow the cells on a bacterial lawn. The intensity of the blue–green lines of the mercury arc, selected with a custom-made band-pass filter, was reduced by neutral-density filters to 1% or less of the normal excitation levels used in fluorescence microscopy of fixed-cell preparations. Fluorescence images of cells were recorded with 0.2 sec exposures to excitation light focused close to the substratum. The images were recorded on a cooled charge-coupled device (CCD) camera (1317×1034) operating in a binning mode (4×4).

To record chemotactic responses, cells cultivated in nutrient medium were incubated in petri dishes for 6 h in starvation buffer, transferred onto a 5×5 cm glass coverslip with a plastic ring, and stimulated with a micropipette filled with 0.1 mM cAMP [2]. Confocal images were taken at intervals of 20 sec on an inverted Zeiss LSM 410 microscope with a 40× Neofluar 1.3 oil-immersion objective. For excitation, the 488 nm argon-ion laser line was used, and the emission collected with a 510–525 nm band-pass filter.

Purification of GFP–actin, polymerization, and in vitro *motility assay*

Cells were harvested from plastic culture plates or shaken suspension cultures and washed once in starvation buffer. The cell pellet was resuspended in four volumes of the following lysis buffer: 10 mM Tris, pH 8.0, 0.5 mM DTT, 30% sucrose, 1 mM PEFA-block, 200 U ml^{-1} aprotinin, 0.5 μg ml^{-1} bestatin, and antipain, leupeptin and pepstatin A (each at 1 μg ml^{-1}; Sigma). Cells were lysed using a Parr bomb at 750 p.s.i. for 30 min at 4°C. The lysate was centrifuged in the cold for 30 min at 10 000 *g* and for 2 h at 100 000 *g*.

Proteins from the 100 000 *g* supernatant were precipitated with 60% ammonium sulfate overnight in the cold, pelleted at 30 000 *g* for 20 min at 4°C, resuspended in 10 ml of G buffer (10 mM Tris, pH 8.0, 0.5 mM sodium ATP, 0.5 mM DTT, 0.2 mM $CaCl_2$, 10 mM benzamidine, 200 mg l^{-1} NaN_3), and dialysed against 2 l of the same buffer for 2 days in the cold. The dialysate was clarified at 100 000 *g* for 1 h at 4°C. Supernatant (5 ml) was loaded onto an FPLC Mono-Q column, and bound proteins separated in 10 mM Tris, pH 8.0, with a 0 to 1 M linear NaCl gradient. The GFP–actin content of the fractions was determined by fluorimetry at 488 nm excitation and 500–520 nm emission. GFP–actin eluted in two fractions between 330 mM and 380 mM NaCl, and was most strongly enriched in the first of these fractions. To further enrich GFP–actin, this fraction was loaded onto a Mono-P column, and bound proteins were eluted in 10 mM Tris, pH 6.8, with a 0 to 1 M linear NaCl gradient. The most strongly enriched of the resulting fractions contained 70–80% GFP–actin.

Actin polymerization was induced by the addition to a final concentration of 100 mM KCl and 2 mM $MgCl_2$, and incubation on ice for 16 h, to either the first fraction alone or a pool of the two fractions. Actin filaments were pelleted at 125 000 *g* for 1 h, and taken up in F buffer (10 mM Tris, pH 8.0, 0.5 mM sodium ATP, 0.2 mM $CaCl_2$, 0.5 mM DTT, 200 mg l^{-1} NaN_3, 100 mM KCl, 2 mM $MgCl_2$). Motility of actin filaments on a surface of heavy meromyosin was measured using the *in vitro* motility assay of Kron *et al.* [17] as adapted by Heidecker *et al.* [23].

Fluorescence microscopy of fixed cells and analytical methods

For labeling of actin in cells with phalloidin, cells producing GFP–actin were cultivated in nutrient medium on glass coverslips, fixed with picric acid/formaldehyde and post-fixed in 70% ethanol according to Humbel and Biegelmann [34]. Specimens were labeled for 30 min with 50–200 ng ml^{-1} of Cy5-phalloidin (courtesy of Heinz Faulstich). Confocal images were taken with a Zeiss LSM 410 microscope using the 488 nm line of an argon-ion laser and a 510–525 nm emission filter for GFP, and the 633 nm line of a helium–neon laser and a 665 nm emission filter for cyanine 5.

To determine the ratio of actin to GFP–actin, proteins separated in 12% SDS–polyacrylamide gels were immunoblotted with [^{125}I]-labeled 236 monoclonal antibody. This antibody was chosen because it bound to an actin fragment comprising amino acids 212–323, far removed from the amino terminus occupied by GFP. The amount of radioactive antibody bound to the 42 kDa and 69 kDa bands was quantified on a Fuji phosphoimager.

Acknowledgements

We thank Richard Albrecht for cooperation, John Murphy for help with image processing and Gerhard Rahn for iodinated antibody. Cy5-phalloidin was a gift from Heinz Faulstich. The work was supported by grant SFB 266/D7 of the Deutsche Forschungsgemeinschaft to G.G.

References

1. Chalfie M, Tu Y, Euskirchen G, Ward WW, Prasher DC: Green fluorescent protein as a marker for gene expression. *Science* 1994, 263:802–805.
2. Gerisch G, Albrecht R, Heizer C, Hodgkinson S, Maniak M: Chemoattractant-controlled accumulation of coronin at the leading edge of ***Dictyostelium*** cells monitored using a green fluorescent protein–coronin fusion protein. *Curr Biol* 1995, 5:1280–1285.
3. Maniak M, Rauchenberger R, Albrecht R, Murphy J, Gerisch G: Coronin involved in phagocytosis: dynamics of particle-induced relocalization visualized by a green fluorescent protein tag. *Cell* 1995, 83:915–924.
4. Waddle JA, Karpova TS, Waterston RH, Cooper JA: Movement of cortical actin patches in yeast. *J Cell Biol* 1996, 132:861–870.
5. Hanakam F, Albrecht R, Eckerskorn C, Matzner M, Gerisch G: Myristoylated and non-myristoylated forms of the pH sensor protein hisactophilin II: intracellular shuttling to plasma membrane and nucleus monitored in real time by a fusion with green fluorescent protein. *EMBO J* 1996, 15:2935–2943.
6. Olson KR, McIntosh JR, Olmsted JB: Analysis of MAP 4 function in living cells using green fluorescent protein (GFP) chimeras. *J Cell Biol* 1995, 130:639–650.
7. Doyle T, Botstein D: Movement of yeast cortical actin cytoskeleton visualized ***in vivo***. *Proc Natl Acad Sci USA* 1996, 93:3886–3891.
8. Segall JE, Gerisch G: Genetic approaches to cytoskeleton function and the control of cell motility. *Curr Opin Cell Biol* 1989, 1:44–50.
9. Schindl M, Wallraff E, Deubzer B, Witke W, Gerisch G, Sackmann E: Cell-substrate interactions and locomotion of ***Dictyostelium*** wild-type and mutants defective in three cytoskeletal proteins: a study using quantitative reflection interference contrast microscopy. *Biophys J* 1995, 68:1177–1190.
10. Condeelis J: Life at the leading edge: the formation of cell protrusions. *Annu Rev Cell Biol* 1993, 9:411–444.
11. Beug H, Katz E, Gerisch G: Dynamics of antigenic membrane sites relating to cell aggregation in ***Dictyostelium discoideum***. *J Cell Biol* 1973, 56:647–658.
12. Spudich A, Wrenn JT, Wessells NK: Unfertilized sea urchin eggs contain a discrete cortical shell of actin that is subdivided into two organizational states. *Cell Motil Cytoskeleton* 1988, 9:85–96.
13. Cao LG, Fishkind DJ, Wang YL: Localization and dynamics of nonfilamentous actin in cultured cells. *J Cell Biol* 1993, 123:173–181.
14. Cubitt AB, Heim R, Adams SR, Boyd AE, Gross LA, Tsien RY: Understanding, improving and using green fluorescent proteins. *Trends Biochem Sci* 1995, 20:448–455.
15. Knecht DA, Loomis WF: Antisense RNA inactivation of myosin heavy chain gene expression in ***Dictyostelium discoideum***. *Science* 1987, 236:1081–1086.

16. De Lozanne A, Spudich JA: Disruption of the ***Dictyostelium*** myosin heavy chain gene by homologous recombination. *Science* 1987, 236:1086–1091.
17. Kron SJ, Toyoshima YY, Uyeda TP, Spudich JA: Assays for actin sliding movement over myosin-coated surfaces. *Methods Enzymol* 1991, 196:399–416.
18. Claviez M, Brink M, Gerisch G: Cytoskeletons from a mutant of ***Dictyostelium discoideum*** with flattened cells. *J Cell Sci* 1986, 86:69–82.
19. Cox D, Ridsdale JA, Condeelis J, Hartwig J: Genetic deletion of ABP-120 alters the three-dimensional organization of actin filaments in ***Dictyostelium*** pseudopods. *J Cell Biol* 1995, 128:819–835.
20. Rubino S, Fighetti M, Unger E, Cappuccinelli P: Location of actin, myosin, and microtubular structures during directed locomotion of ***Dictyostelium*** amoebae. *J Cell Biol* 1984, 98:382–390.
21. Weber I, Wallraff E, Albrecht R, Gerisch G: Motility and substratum adhesion of ***Dictyostelium*** wild-type and cytoskeletal mutant cells: a study by RICM/bright-field double-view image analysis. *J Cell Sci* 1995, 108:1519–1530.
22. Heim R, Tsien RY: Engineering green fluorescent protein for improved brightness, longer wavelengths and fluorescence resonance energy transfer. *Curr Biol* 1996, 6:178–182.
23. Heidecker M, Yan-Marriott Y, Marriott G: Proximity relationships and structural dynamics of the phalloidin binding site of actin filaments in solution and on single actin filaments on heavy meromyosin. *Biochemistry* 1995, 34:11017–11025.
24. Rizzuto R, Brini M, De Giorgi F, Rossi R, Heim R, Tsien RY, Pozzan T: Double labelling of subcellular structures with organelle-targeted GFP mutants ***in vivo***. *Curr Biol* 1996, 6:183–188.
25. Holmes KC, Popp D, Gebhard W, Kabsch W: Atomic model of the actin filament. *Nature* 1990, 347:44–49.
26. Schröder RR, Manstein DJ, Jahn W, Holden H, Rayment I, Holmes KC, Spudich JA: Three-dimensional atomic model of F-actin decorated with ***Dictyostelium*** myosin S1. *Nature* 1993, 364:171–174.
27. Rayment I, Holden HM, Whittaker M, Yohn CB, Lorenz M, Holmes KC, Milligan RA: Structure of the actin–myosin complex and its implications for muscle contraction. *Science* 1993, 261:58–65.
28. Kreitmeier M, Gerisch G, Heizer C, Müller-Taubenberger A: A talin homologue of ***Dictyostelium*** rapidly assembles at the leading edge of cells in response to chemoattractant. *J Cell Biol* 1995, 129:179–188.
29. Hawkins M, Pope B, Maciver SK, Weeds AG: Human actin depolymerizing factor mediates a pH-sensitive destruction of actin filaments. *Biochemistry* 1993, 32:9985–9993.
30. Haugwitz M, Noegel AA, Rieger D, Lottspeich F, Schleicher M: ***Dictyostelium discoideum*** contains two profilin isoforms that differ in structure and function. *J Cell Sci* 1991, 100:481–489.
31. Gottwald U, Brokamp R, Karakesisoglou I, Schleicher M, Noegel AA: Identification of a cyclase-associated protein (CAP) homologue in ***Dictyostelium discoideum*** and characterization of its interaction with actin. *Mol Biol Cell* 1996, 7:261–272.
32. Faix J, Gerisch G, Noegel AA: Overexpression of the csA cell adhesion molecule under its own cAMP-regulated promoter impairs morphogenesis in ***Dictyostelium***. *J Cell Sci* 1992, 102:203–214.
33. Häder DP, Claviez M, Merkl R, Gerisch G: Responses of ***Dictyostelium discoideum*** amoebae to local stimulation by light. *Cell Biol Int Rep* 1983, 7:611–616.
34. Humbel BM, Biegelmann E: A preparation protocol for postembedding immunoelectron microscopy of ***Dictyostelium discoideum*** cells with monoclonal antibodies. *Scanning Microsc* 1992, 6:817–825.
35. Vandekerckhove J, Weber K: Vegetative ***Dictyostelium*** cells containing 17 actin genes express a single major actin. *Nature* 1980, 284:475–477.
36. Romans P, Firtel RA: Organization of the actin multigene family of ***Dictyostelium discoideum*** and analysis of variability in the protein coding regions. *J Mol Biol* 1985, 186:321–335.

Because *Current Biology* operates a 'Continuous Publication System' for Research Papers, this paper has been published via the internet before being printed. The paper can be accessed from http://biomednet.com/cbiology/cub.htm – for further information, see the explanation on the contents page.